Electronic Supplementary Material (ESI) for Catalysis Science & Technology.

Propane oxidative dehydrogenation using CO_2 over CrO_x/Fe-CeO_2 catalysts

Hedun Wang [a], Thu D. Nguyen [a] and George Tsilomelekis [a]*

[1]Department of Chemical and Biochemical Engineering, Rutgers, The State University of New Jersey, Piscataway, NJ 08854, USA.

Supporting Information

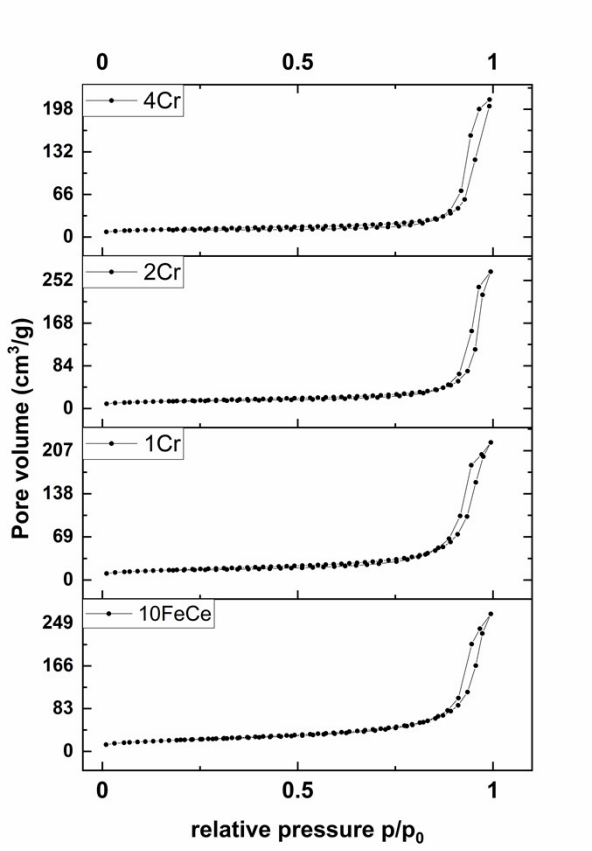

Figure S 1: Adsorption isotherms of the 10Fe-CeO_2 support and nCr/10Fe-CeO_2 catalysts with various Cr loadings.

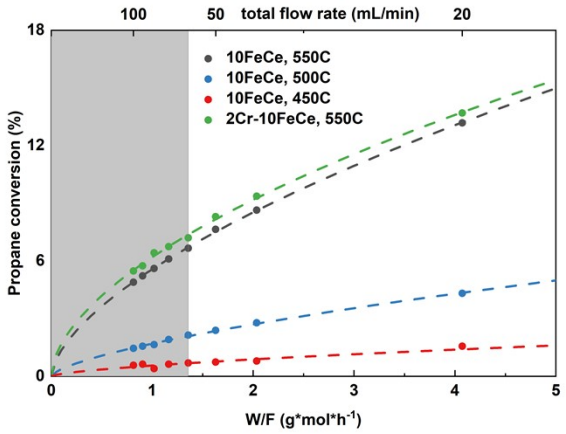

Figure S 2: Test for kinetic regime identification and elimination of external mass transfer limitation. All tests were performed at 823K, varying flowrate from 20mL/min to 100mL/min with constant propane and CO2 partial pressure.

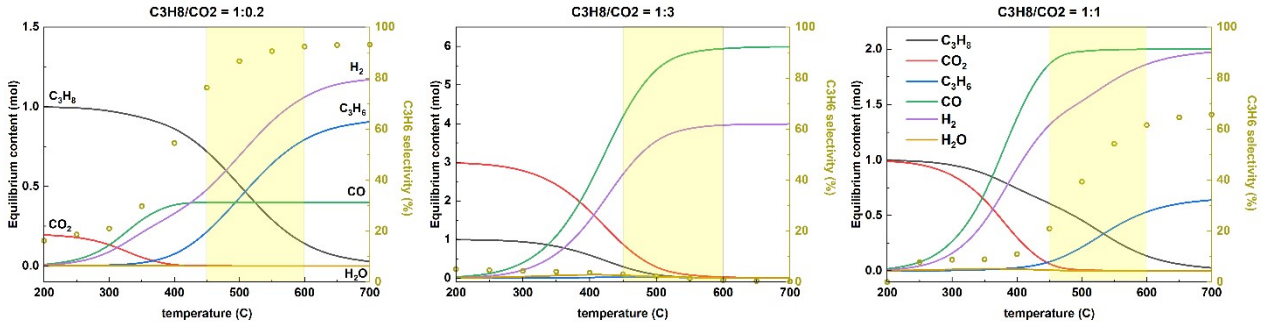

Figure S 3: Thermodynamic predictions of temperature-dependent equilibrium composition with propane and carbon dioxide as initial state with different relative partial pressures.

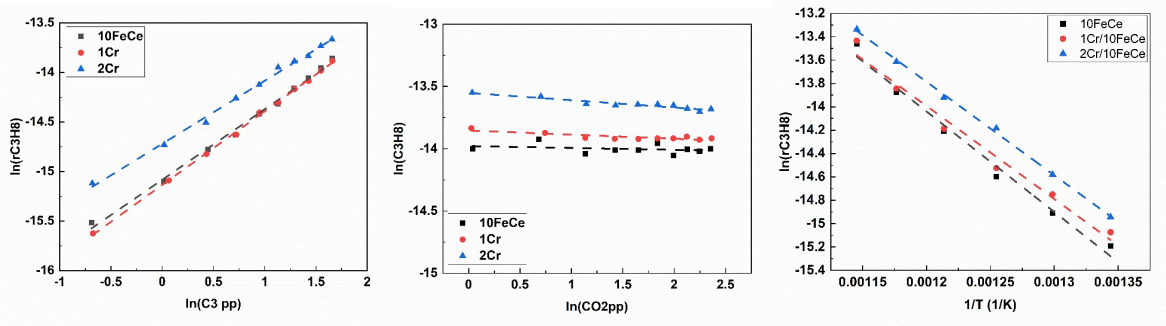

Figure S 4: Log-log plot of propane consumption rate as a function of C_3H_8 and CO_2 partial pressure; Arrhenius plot.

Power-law kinetics and apparent reaction orders

Kinetic model details and parameters

The kinetic model developed based on the following reactor and reaction condition assumptions. (1) Reactions are performed at low propane conversion (<10%) in order to guarantee differential reactor conditions. (2) Intrinsic kinetic conditions were ensured by adjusting the total mass flow rate of the feed at constant C_3H_8 and CO_2 partial pressure. (3) Carbon balance is a key point to ensure also the accuracy of kinetic analysis and parameter regression[1]. In this work, carbon balance of all individual experiments maintained at level above 99.4%. (4) Volumetric flow from upstream and downstream of the reactor was regarded equivalent due to the excess feed of inert gas (over 90% in most cases) and low conversion of reactants in the kinetic regime.

All relevant steps are shown in the main manuscript. The proposed steady-state kinetic model assumes: (1) Two types of active sites (identified from previous works[2-5]), i.e. surface active oxygen sites (S_1) and oxygen vacancies (S_2). (2) No migrations of adsorbed intermediates between S_1 and S_2 sites. (3) Single site adsorption. (4) Langmuir-Hinshelwood Hougen-Watson (LHHW) surface reaction mechanism was applied to describe the reaction networks composed of PDH, DRF and RWGS assuming a primary rate-limiting step (p-rds) and two secondary rate-limiting steps (s-rds).

It should be noted that in the elementary steps, S_1 and O_S_2 are considered as equivalent, but distinct. Similarly, the H_S_1 and OH_S_2 as well as CH_x_S_1 and CH_xO_S_2 are regarded as 'redox pairs' that represent the overall oxygen removal and replenishment processes during the reaction. In addition, S_1 and S_2 sites are inter-convertible in these elementary steps and total amount of site ($S_{1,tot}$ and $S_{2,tot}$) are in dynamic equilibrium.

Site balance:

$$\frac{S_{1,tot}}{S_1} = (1 + \frac{S_{1,C_3H_7}}{S_1} + \frac{S_{1,H}}{S_1} + \frac{S_{1,CH}}{S_1} + \frac{S_{1,CH_3}}{S_1} + \frac{S_{1,CH_3CH}}{S_1})$$

$$\frac{S_{2,tot}}{S_2} = (1 + \frac{S_{2,COOH}}{S_2} + \frac{S_{2,OH}}{S_2} + \frac{S_{2,CHO}}{S_2} + \frac{S_{2,CH_3O}}{S_2} + \frac{S_{2,CH_2O}}{S_2})$$

Assuming highly reactive and unstable surface adsorbates including CH, CH_3, CH_3CH, CH_3O and CH_2O, the site balance were simplified to:

$\frac{S_{1,tot}}{S_1} = (1 + \frac{S_{1,C_3H_7}}{S_1} + \frac{S_{1,H}}{S_1})$, and $\frac{S_{2,tot}}{S_2} = (1 + \frac{S_{2,COOH}}{S_2} + \frac{S_{2,OH}}{S_2} + \frac{S_{2,CHO}}{S_2})$

The reactor design equation is:

$$r_{C_3H_8} = \frac{dX_{C_3H_8}}{d(W/F_{C_3H_8})}$$

$$= \frac{\partial X_{C_3H_8}}{d\left({}^{W}/_{(F_{tot}P_{C_3H_8})}\right)} \cong \frac{\Delta X_{C_3H_8}}{\Delta\left({}^{W}/_{(F_{tot}P_{C_3H_8})}\right)} = \frac{X_{C_3H_8,final} - X_{C_3H_8,ini}}{\left({}^{W}/_{(F_{tot}P_{C_3H_8})}\right)_{final} - \left({}^{W}/_{(F_{tot}P_{C_3H_8})}\right)_{ini}}$$

Assuming s14 as primary rate-limiting step, s1 and s4 as secondary rate-limiting step, overall PDH, DRF and RWGS rates were expressed as:

$$r_{DH} = \frac{k_{DH}\left(P_{C_3H_8}P_{H_2}^{-1/2} - \frac{P_{C_3H_6}P_{H_2}^{1/2}}{K_{DH}}\right)}{\left[1 + K_2^{-1}P_{C_3H_6}\left(K_{H_2}P_{H_2}\right)^{0.5} + \left(K_{H_2}P_{H_2}\right)^{0.5}\right]}$$

$$r_{RWGS} = \frac{k_{RWGS}\left(P_{CO_2}^{2}P_{CO}^{-2}P_{H_2} - \frac{P_{H_2O}}{K_{RWGS}}\right)}{\left(1 + K_5P_{CO_2}\left(K_{H_2}P_{H_2}\right)^{0.5}\left(1 + \frac{K_5}{P_{CO}}\right) + \frac{K_{CHO}P_{C_3H_6}^{1/3}P_{CO_2}}{P_{CO}\left(P_{H_2}\right)^{\frac{1}{2}}}\right)^2}$$

$$r_{DRF} = \frac{k_{DRF}\left[P_{C_3H_8}^{1/3}P_{CO_2}P_{CO}^{-1}P_{H_2}^{-5/6} - \frac{P_{CO}P_{H_2}^{1/2}}{K_{DRF}}\right]\left[1 + K_2^{-1}P_{C_3H_6}\left(K_{H_2}P_{H_2}\right)^{0.5} + \left(K_{H_2}P_{H_2}\right)^{0.5}\right]^{-1}}{1 + K_5P_{CO_2}\left(K_{H_2}P_{H_2}\right)^{0.5}\left(1 + \frac{K_5}{P_{CO}}\right) + \frac{K_{CHO}P_{C_3H_6}^{1/3}P_{CO_2}}{P_{CO}\left(P_{H_2}\right)^{\frac{1}{2}}}}$$

In the kinetics rate expression of DH, RWGS and DRF, all lumped parameters are shown below:

$$k_{DH} = k_2S_{1,tot}K_{C_3H_8}K_{H_2}^{-1/2}$$

$$K_{DH} = \frac{K_{C_3H_8}}{K_2^{-1}K_{H_2}}$$

$$k_{RWGS} = k_7S_{2,tot}^{2}K_5^2K_{H_2}K_6^2$$

$$K_{RWGS} = \frac{K_5^2K_{H_2}K_6^2}{K_{H_2O}}$$

$$k_{DRF} = k_{14} S_{1,tot} S_{2,tot} K_{CHO} K_{C_3H_8}^{1/3} K_4 K_{H_2}^{-5/6}$$

$$K_{DRF} = K_{14} K_{CHO} K_4 K_{H_2}^{-5/6}$$

$$K_{CHO} = \left(K_8 K_9 K_{10}^2 K_{11} K_{12}^2 K_{13}^2\right)^{1/3} K_4 K_{C_3H_8}^{1/3} K_{H_2}^{-1/2}$$

It should be noted that the derived expressions lumped all possible parameters from elementary steps and site balances. While K_2, K_5 and K_6 stands for the equilibrium constants for each elementary step, most other constants are dismissed from the final expression, due to either the fact that rate-limiting steps are not considered to approach their equilibrium, or the equilibrium constants are essentially lumped together. Details of lumped parameters could be found in the supporting information. PDH equilibrium constant was expressed as[70] $K_{DH} = exp(16.858 - 15934/T + 148728/T^2)$, RWGS equilibrium constant was expressed as[71] $K_{RWGS} = 10\text{^}(2.4198 - 0.0003855 * T + 2180.6/T)$ and dry reforming equilibrium constant K_{DRF} is considered much larger in the order of magnitude than partial pressure terms on the numerator according to thermodynamic equilibrium examination in the supporting information Figure S4. Reaction rate constants k_{rxn} and adsorption constants for certain reaction components K_i (i stands for component appeared in the reaction system, both reactants and products) were expressed by linearized Arrhenius equation and linearized van-Hoff equation with a reference temperature at 550°C (823K):

$$k_{rxn} = k_{rxn,0}\left(\frac{-Ea_{rxn}}{R}\left(\frac{1}{T} - \frac{1}{T_r}\right)\right)$$

$$K_{cpn} = K_{cpn,0}\left(\frac{-\Delta H_{cpn}}{R}\left(\frac{1}{T} - \frac{1}{T_r}\right)\right)$$

For all parameters to be fitted, the initial values arose from several different DFT calculations[59, 62, 72, 73] on propane dehydrogenation and dry reforming reactions. Kinetic data was fitted via MATLAB nonlinear regression function and model accuracy was optimized by maximizing adjusted R squared:

$$R^2 = 1 - \frac{RSS}{TSS} = 1 - \frac{\sum (r_{exp} - r_{cal})^2}{\sum (r_{exp} - \bar{r}_{exp})^2}$$

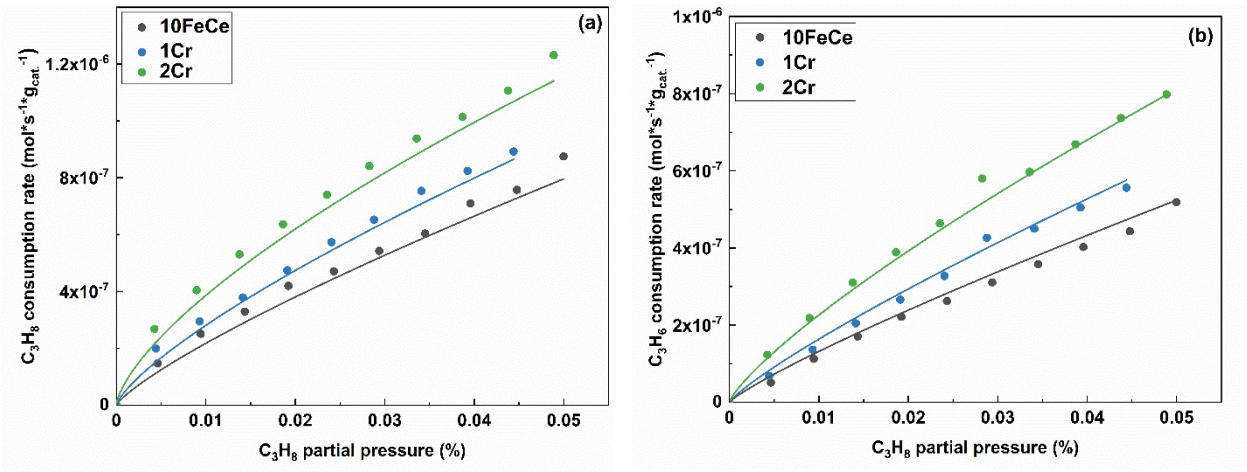

Figure S 5: Model prediction of propane consumption rates (a) and propylene formation rates (b) at 550oC with 100mL/min total flow, varying the propane partial pressure from 0.5% to 5%.

References

[1] C.A. Carrero, R. Schloegl, I.E. Wachs, R. Schomaecker, Critical Literature Review of the Kinetics for the Oxidative Dehydrogenation of Propane over Well-Defined Supported Vanadium Oxide Catalysts, ACS Catalysis 4 (2014) 3357-3380. 10.1021/cs5003417.

[2] H. Wang, G. Tsilomelekis, Catalytic performance and stability of Fe-doped CeO2 in propane oxidative dehydrogenation using carbon dioxide as an oxidant, Catalysis Science & Technology (2020). 10.1039/d0cy00586j.

[3] H.-X. Fan, J. Feng, W.-Y. Li, Promotional effect of oxygen storage capacity on oxy-dehydrogenation of ethylbenzene with CO2 over κ-Ce2Zr2O8(111), Applied Surface Science 486 (2019) 411-419. 10.1016/j.apsusc.2019.04.244.

[4] A. Hezam, K. Namratha, Q.A. Drmosh, D. Ponnamma, J. Wang, S. Prasad, M. Ahamed, C. Cheng, K. Byrappa, CeO2 Nanostructures Enriched with Oxygen Vacancies for Photocatalytic CO2 Reduction, ACS Applied Nano Materials 3 (2019) 138-148. 10.1021/acsanm.9b01833.

[5] E. Nowicka, C. Reece, S.M. Althahban, K.M.H. Mohammed, S.A. Kondrat, D.J. Morgan, Q. He, D.J. Willock, S. Golunski, C.J. Kiely, G.J. Hutchings, Elucidating the Role of CO2 in the Soft

Oxidative Dehydrogenation of Propane over Ceria-Based Catalysts, ACS Catalysis 8 (2018) 3454-3468. 10.1021/acscatal.7b03805.